Orbital: The Electronic Journal of Chemistry
journal homepage: www.orbital.ufms.br
e-ISSN 1984-6428

| Vol 10 | | No. 7 | | October-December 2018 |

FULL PAPER

Cassava Starch-Based Films Reinforced with Clay Minerals

Elthon Ferreira Passos[a], Rafael Marangoni[a], and Leandro Zatta[b]

[a]Laboratory of Materials and Inorganic Compounds - LabMat, Department of Chemistry, State University of Central-West, 85040-080, Guarapuava, Paraná, Brazil.
[b]Department of Chemistry, Federal Technological University of Paraná, 85503-390, Pato Branco, Paraná, Brazil.

Article history: Received: 19 April 2018; revised: 08 September 2018; accepted: 25 October 2018. Available online: 31 December 2018. DOI: http://dx.doi.org/10.17807/orbital.v10i7.1171

Abstract:

This paper presents the obtaining and characterization of starch-based polymeric films with the addition of kaolinite, montmorillonite and a commercial clay as filler, glycerol was used as plasticizer. The materials were characterized by X-ray diffraction, Fourier transform infrared spectroscopy, scanning electron microscopy, energy-dispersive X-ray spectroscopy, thermogravimetry, mechanical properties, colorimetry and water solubility. It was generally found that the addition of the clay minerals to the polymer matrices altered the evaluated properties of the materials. The films containing the clay minerals presented lower temperatures of occurrence of the thermal events, greater capacity of elongation, lower rupture tension and greater resistance to water solubility. The film containing the commercial clay stands out for presenting red coloration, due to the presence of iron contents in the clay composition. The films synthesized from cassava starch with the addition of glycerol and natural origin clay minerals obtained in this work demonstrated interesting properties for technological applications.

Keywords: biopolymers; (nano)composites; clay minerals; cassava starch

1. Introduction

The development and production of polymer materials has gained increased attention in the last decades due to the interesting properties of this class of materials, as well as the vast area of application, especially in the food, pharmaceutical, packaging and agricultural industry among others [1, 2]. Due to the increasing demand of these materials, concerns have arisen regarding the environmental impacts, mainly in relation to exposure to the environment, that motivates the research for materials obtained from alternative precursors that present the properties of conventional polymers and are environmentally friendly [3, 4].

In this context, the biopolymers stand out, this class of materials can be degraded by microorganisms and enzymes when discarded, contributing to the reduction of the amount of solid residues of difficult degradation [2, 4, 5].

The most studied biodegradable polymers are produced from natural and renewable sources found in abundance in nature. An example of a biodegradable polymer precursor is the starch, which is present in some classes of plants and is responsible for its energy reserve [6].

Starch is composed of amylose and amylopectin, which are constituted of interconnected D-glucose monomer units. Amylose is a linear polymer composed of α 1→4 bonds, whereas amylopectin has a branched structure composed of α 1→6 bonds. The content of these compounds may vary according to the source of starch [6, 7].

The polymer obtained from the processing of pure starch presents important characteristics, the most important is its biodegradability. However, the applicability of starch is restricted, mainly due to its low mechanical resistance [8]. To improve, or modify, the characteristics of the polymeric material obtained from starch, the

*Corresponding author. E-mail: elthonpassos.quimica@gmail.com

addition of reinforcing agents is necessary, which act on the optical, mechanical and physicochemical properties of the materials, for example [9].

The glycerol (from the family of polyols) is among the most widely used additives in the production of starch-based biopolymers, this compound acts as a plasticizer, making the final material more flexible and with better workability [7, 10, 11].

Clay minerals are a class of materials that is widely used in the polymer industry, as it provides significant improvements in mechanical, optical, thermal and other properties [2]. The use of clay minerals together with the polymeric matrix formed by the starch-glycerol system motivates the obtaining of materials with different properties and possible to dispose of in the environment, due to the biodegradability and by the fact that the clays are obtained from the soil [12].

Extremely abundant, clays are characterized by low granulometry, non-toxicity, high surface area, low cost and high potential of application in the development of technological products, being able to be applied in different classes of materials [13].

This work aims to synthesize and characterize biopolymer films based on cassava starch, with the addition of glycerol as a plasticizer and three different clay minerals as filler, being kaolinite (high purity), montmorillonite (international standard) and a natural clay used in the western region of Santa Catarina State - Brazil, which is composed of significant amounts of kaolinite and montmorillonite.

2. Results and Discussion

The obtained films were named according to their composition: SG = starch/glycerol; SG-k = starch/glycerol/kaolinite; SG-m = starch/glycerol/montmorillonite; SG-sm3 = starch/glycerol/sm3.

The Fourier Transform infrared spectroscopy (FTIR) spectra of the clay and SG, SG-k, SG-m and SG-sm3 films are shown in Figure 1, while the assignments of the vibrations are described in Table 1. The spectra of clays and SG film are shown in each figure for comparison.

In general, was observed in the FTIR spectra of the films with the addition of clays as a filler, changes in the profile of two characteristic vibrations of the polymer matrix, being 480 and 524 cm^{-1} for C-H bonds and of the phenyl ring vibrations, respectively [14–17]. These vibrations are possibly overlaid with the Al–O, Si–O and Mg–O (lattice) vibrations of the clays.

The FTIR spectrum of the SG-k sample (Figure 1b.) shows the vibrations related to the surface and internal hydroxyls of kaolinite in 3692 and 3617 cm^{-1} (Figure 1c.), respectively [18], are present in the spectrum of the film, attesting to the presence of clay in the same, however, these vibrations are shown with low intensity, probably because of the low content of clay added in relation of the polymer matrix. The vibration at 468 cm^{-1}, for the Si–O–Si flexion [19], which is characteristic of kaolinite, is also present in the SG-k spectrum, indicating the presence of clay in the film.

The FTIR spectrum related to the incorporation of montmorillonite in the film (Figure 1d.), shows that the vibrations at 468 and 802 cm^{-1}, which are characteristic of montmorillonite [19] (Figure 1e.) related to Si-O-Si bending and the presence of amorphous silica, respectively, are visualized in the spectrum of the SG-m film, suggesting that the clay is dispersed in the polymer matrix of this film, as expected.

The film containing the sm3 clay (SG-sm3), shown in Figure 1f., presented similar characteristics to the films containing the clay minerals kaolinite (Figure 1b.) and montmorillonite (Figure 1d.), SG-k and SG-m, respectively. The vibrations at 468 and 802 cm^{-1} (Figure 1g.) attests to the presence of clay in the SG-sm3 film. The sm3 samples, clay and film fillered with sm3, have red color due to the presence of Fe^{3+} cations in the clay and the presence of this ion is identified by the vibration at 432 cm^{-1}, which refers to the Si–O–Fe vibration, characteristic of some clay minerals [20].

In general, the FTIR analysis suggests that, in all films, the different clay minerals were dispersed in the polymer matrix. This observation is attested by the presence of bands characteristic of the clay minerals, visualized in the film spectra even at low intensity, indicating

that the clay minerals are diluted in the polymer matrix. Another consideration is that, in all the films in which the clays were added, the characteristic vibrations of the polymer matrix did not present substantial displacements or changes, indicating the structural preservation of the polymer characteristics.

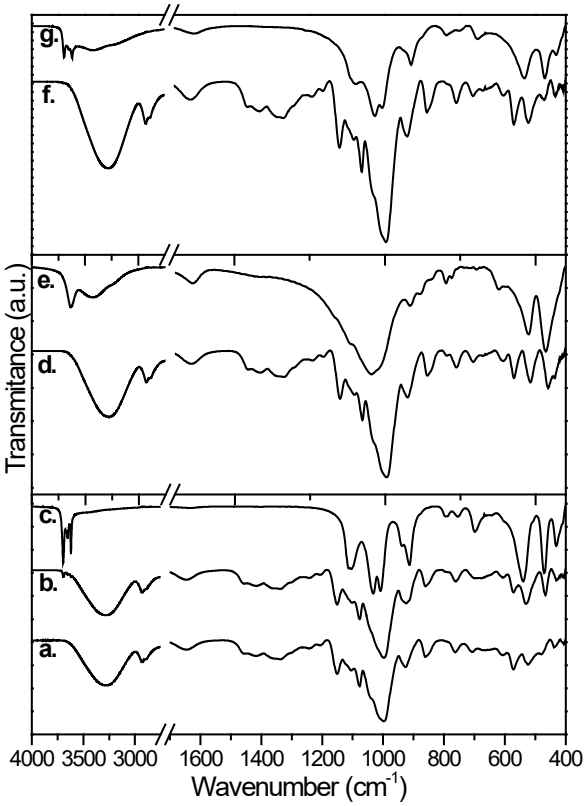

Figure 1. FTIR spectra for a. SG; b. SG-k; c. kaolinite; d. SG-m; e. montmorillonite; f. SG-sm3; g. sm3 clay.

The films were characterized by X-ray diffraction (XRD), shown in Figure 2, and was verified that the SG film has a characteristic amorphous reflection for polymers in the region between 12-27° (2θ). In this same region, three others reflections at 17.08°, 21.14° and 23.54° (2θ) of considerable intensity were verified, which could possibly be due to the crystalline regions of the films where the polymer chains are structurally organized [21].

By analyzing the diffractograms of the films containing the clays (Figure 2), the permanence of the previously mentioned reflections in the region between 12-27° (2θ), characteristic of the polymer matrix, was verified. In general, the film SG-k was the only sample that presented significant differences in the X-ray diffractogram pattern, in comparison to the SG film (Figure 2a), where characteristic reflections of the (001) and (002) planes of the kaolinite clay are verified [22, 23]. However, these reflections are displaced at lower angles of diffraction relative to pure clay, indicating expansion of the observed crystallographic planes, probably because of the interaction between the highly hydroxylated polymer chains with the also highly hydroxylated surface of the kaolinite crystals, which causes structural distortions in this clay. The interplanar basal distance of the kaolinite calculated by Bragg's law, was 7.13 Å, while the values for the same reflections, but for the composite, in the polymer matrix is 7.43 Å.

Table 1. Assignment of the main vibrations observed in Figure 1 [14–20].

Assignment	Wavenumber (cm^{-1})	Sample
–OH, hydroxyl stretching	3698	kaolinite, sm3
	3653	kaolinite
	3631	montmorillonite
	3617	kaolinite, sm3
*O-H, stretch	3278	SG, SG-k, SG-m, SG-sm3
*C–H, stretch	2935	SG, SG-k, SG-m, SG-sm3
*C=O, starch-related stretching	1644	SG, SG-k, SG-m, SG-sm3
*polysaccharide vibrations	1200–1000	SG, SG-k, SG-m, SG-sm3
Si-O, stretch	1101	sm3
*C–H, rocking	~920	SG, SG-k, SG-m, SG-sm3
*C–O–H, bending	~860	SG, SG-k, SG-m, SG-sm3
amorphous silica	800	kaolinite, montmorillonite, sm3
*C–O–C of the ring	764	SG, SG-k, SG-m, SG-sm3
*C–H out of plane bending	708	SG, SG-k, SG-m, SG-sm3
*C–H out of plane bending	573	SG, SG-k, SG-m, SG-sm3
Si–O–Al	541	kaolinite
Si–O–Al	536	kaolinite
Si–O–Al	524	montmorillonite
*phenyl ring	524	SG, SG-k, SG-m, SG-sm3
*C–H vibration	480	SG
Si–O–Si, bend	468	kaolinite, sm3
Si–O–Si, bend	464	montmorillonite
Si –O–Fe	432	kaolinite, sm3

*vibration of the polymeric matrix

For the addition of montmorillonite and sm3 clays Figures 2b and 2c, respectively, the same effects of kaolinite addition are not verified, possibly due to the surface of the kaolinite, which is highly hydroxylated (Al-OH and silanol-Si-OH groups), whereas montmorillonite exhibits its surface with Si-O-Si groups, resulting in the random dispersion through polymer matrix. In relation to the sm3 clay, it is composed mainly by montmorillonite, leading to the same consideration made for the SG-m film. The absence of characteristic reflections of the clay minerals in the SG-m and SG-k films indicates the possible occurrence of the delamination process of the clays in the polymer matrix.

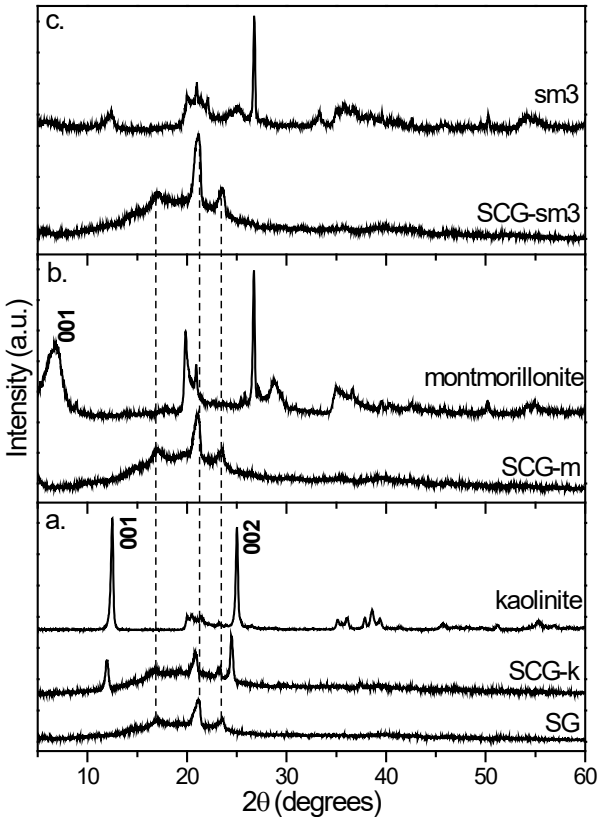

Figure 2. X-ray diffractograms for a. SG, SG-k and kaolinite; b. SG-m and montmorillonite; c. SG-sm3 and sm3 clay.

The films were characterized by scanning electron microscopy (SEM) and the micrographs are shown in Figure 3.

The SG film (Figure 3a) presented a smooth and homogeneous surface, and the regions that indicate another phase (white spots in the micrograph) are attributed to the presence of impurities in the material, probably from the contaminants present in the glassware used in the synthesis and/or drying process by the release of particles from the walls of the oven during the drying process.

For the micrograph of the SG-k film, Figure 3b, kaolinite crystals of considerable size and high concentration regions are found in the film, possibly reflecting the presence of the kaolinite characteristic peaks observed in the X-ray diffraction (Figure 2b).

The micrographs of the SG-m and SG-sm3 films, Figures 3c and d, shown better dispersion of the clay minerals in comparison to the kaolinite, possibly due to the delamination process of the montmorillonite and sm3 clays in the polymer matrix, as discussed for XRD analysis (Figure 2). In the SG-sm3 film, larger crystals are observed in relation to the SG-m film, probably due to the presence of different minerals in the composition of the sm3 clay.

The films were characterized by EDS (Table 2), the results are shown in atomic percentage.

Table 2. Composition of the films (% atomic) determined by EDS.

Element (%)	SG-k	SG-m	SG-sm3
Carbon	98.905	99.215	99.109
Aluminum	0.511	0.258	0.288
Silicon	0.583	0.527	0.452
Iron	-	-	0.150

From the data shown in Table 2, it was verified that all the films presented contents of the elements aluminum and silicon, indicating the presence of the added clays in the polymer films. The SG-sm3 film is characterized by the fact that it presents iron content, which corroborates with what was observed by the infrared spectroscopy technique (Figure 1, Table 1).

The influence of the clay minerals in relation to the thermal behavior of the films was verified, the samples were submitted to thermogravimetric analysis (TGA) and differential thermal analysis (DTA). The thermograms are shown in Figure 4, while Table 3 shows the temperatures of the events and the residue levels after the thermal degradation of the films.

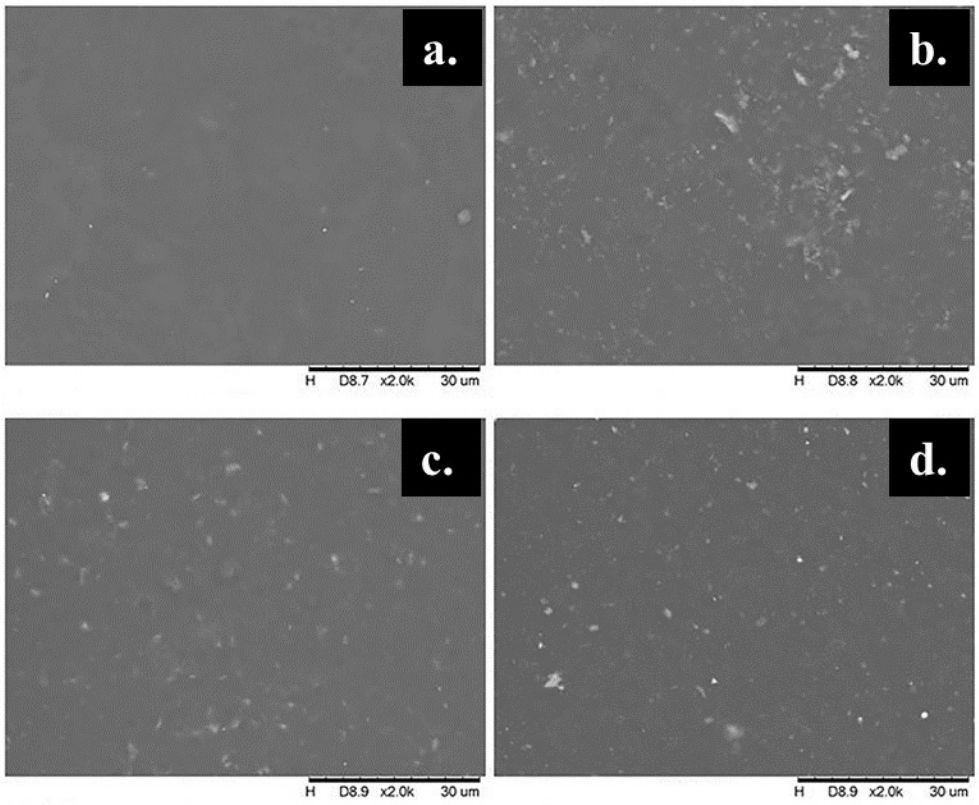

Figure 3. Scanning electron micrographs of the films: a. SG; b. SG-k; c. SG-m and d. SG-sm3. All figures are shown with 2000x magnifications.

It was observed in all thermograms that there was a humidity loss around 70 °C, this event is also evidenced by an endothermic peak in the same region of the DTA curves [24]. By the analysis of SG DTA curve (Figure 4 b), it is observed an endothermic peak at 319 ºC, which refers to the thermal decomposition of the starch. For the films with the addition of clay minerals, the same event occurs, however, at temperatures below 319 °C, as shown in Table 3.

For the SG film (Figure 4a), a second stage of degradation of the organic matrix is verified, evidenced by an exothermic peak in the DTA curve in the region of 590 °C [24]. This event is not observed in the SG-k and SG-m films; however, for the SG-sm3 film, the same thermal degradation profile is observed, but this second event occurs at 477 °C, a lower temperature compared to the same event in the SG film.

In general, the obtained results regard to the thermal behavior of the composites are similar to the observed in the literature for films of the system based on *cará* starch/glycerol/layered compounds, where kaolinite was the filler, and the presence of this clay not provided greater resistance to the thermal degradation in the material [25]. The addition of clays such as kaolinite and montmorillonite in polymeric systems, similar to that evaluated in this work, leads to higher temperatures for the thermal events and the variation in relation to the film without fillers depends on properties such as particle size, dispersion heterogeneity, added charge content and type of species intercalated in the clay [26-28]. As verified by the scanning electron micrographs of the nanocomposites (Figure 3), the samples present regions with considerable concentration of the added clay fillers, indicating an irregular dispersion in the polymeric matrix. This observation possibly contributes to the slightly lower temperatures of occurrence in the observed thermal events compared to the SG film, contrary to the behavior generally observed in the literature [27-29].

The most significant temperature reduction in starch degradation around 320 °C (SG film) was for the film containing the kaolinite (SG-k), the presence of this clay led to at a lower temperature degradation. This behavior may be

interesting in relation to the disposal of the material into the environment.

For the sample SG-sm3, because the sm3 clay is composed mainly of a mixture of kaolinite and montmorillonite (and others minerals), the thermal events were expected to occur in intermediates temperatures in relation to SG-k and SG-m films. The presence of the second thermal event in the SG-sm3 DTA curve (Figure d) similar to the SG film is possibly due to weaker interactions between the sm3 clay and the polymer matrix compared to the other clays evaluated.

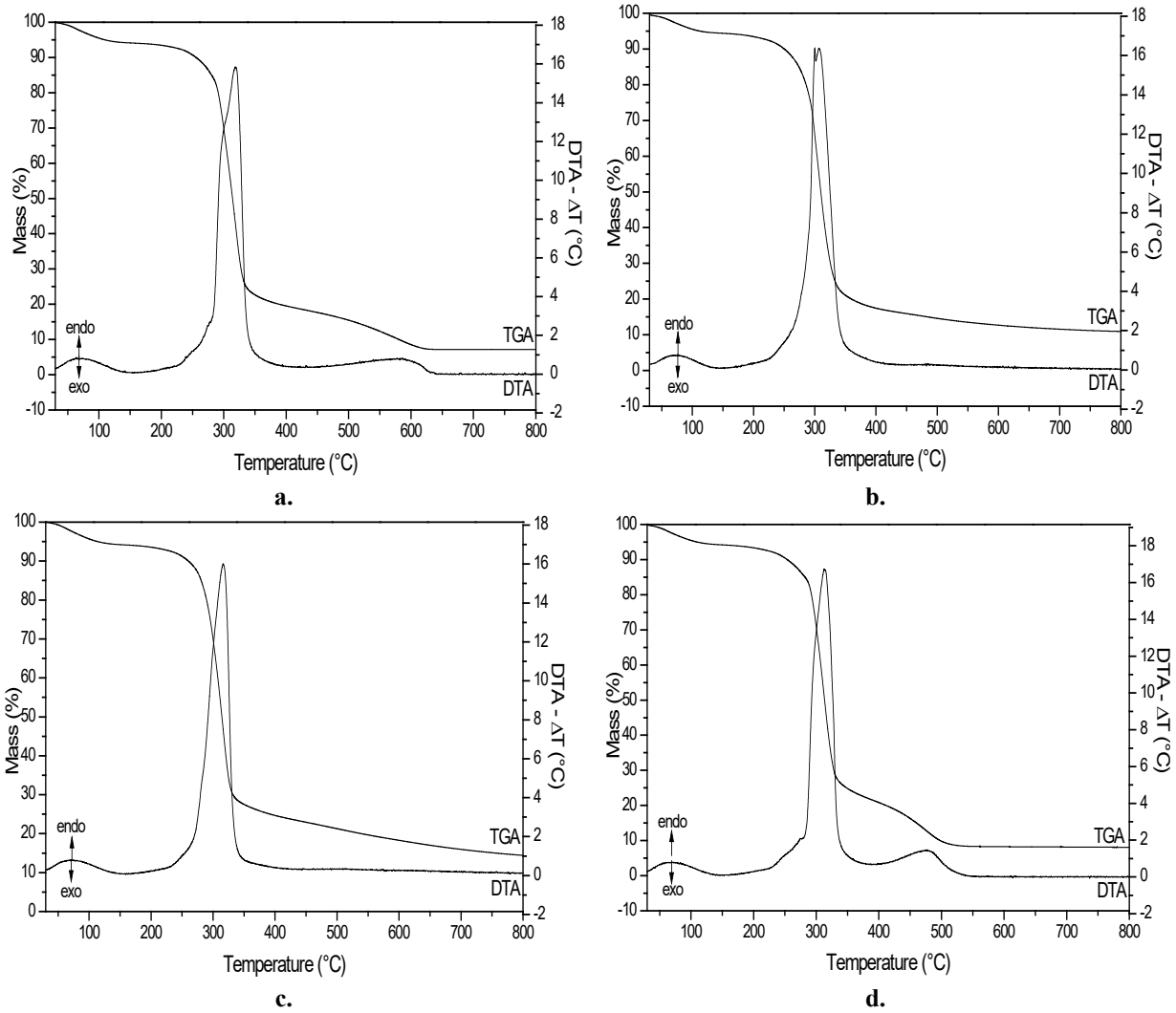

Figure 4. Thermal analysis curves (TGA/DTA) for a. SG, b. SG-k, c. SG-m and d. SG-sm3.

Table 3. Temperatures of the thermal events of the samples.

Film	Humidity loss (°C)	Decomposition (°C)
SG	75	319
SG-k	76	307
SG-m	72	316
SG-	70	312

The films were analyzed in relation to thickness and mechanical properties. The thickness data is shown in Table 4, while the Young's modulus (*E*) and ultimate tensile strength (σ_u) data are shown in Figure 5 and Table 4. The elasticity and maximum tensile stress of the films containing clay minerals were compared to the film without addition of filler, showing the effect of the presence of the clays in these properties, the comparison of the data is shown in Table 4 (%*E* and %σ_u).

In relation to the thickness of the films, the addition of kaolinite and montmorillonite, compared to the SG film, no significantly change in the value of this property was observed, however, when the sm3 charge was added, the film SG-sm3 had the greater thickness in relation

to the others.

Analyzing the data of Table 4 and Figure 5a., is observed by the difference between the Young's modulus values of the clay-containing films with the SG film, %*E*, that the addition of the fillers contributed to an significant change in this property, since the values obtained indicated a greater elongation capacity in these films. The film reinforced with kaolinite (SG-k) stands out among the others materials, since it showed a gain of 14.84%, while the film containing montmorillonite (SG-m) showed a difference of 11.53%, followed by the SG-sm3 sample, which presented a gain of 10.47%.

For the property of ultimate tensile strength, σ_u, the observed values, in all cases, presented a decrease in relation to the SG film (Table 4, Figure 5b.). The film reinforced with the sm3 clay presented a smaller decrease of 6.96%. The addition of kaolinite provided a decrease of 23.00% while that of montmorillonite 32.28%. The results for this property show that the addition of the clay minerals makes the evaluated polymer films more easily brittle.

The smaller decrease in the σ_u for the SG-sm3 film, compared to the SG film, indicates that clay has low interaction with the polymer matrix, possibly due to its composition. The result for this mechanical property reinforces the proposed assumption for the thermal behavior of the SG-sm3 film as discussed for TGA/DTA techniques. Comparing the $\%\sigma_u$ values of the SG-k and SG-m films, the latter presented a higher value, possibly due to the better dispersion of montmorillonite, as observed in the SEM technique (Figure 3).

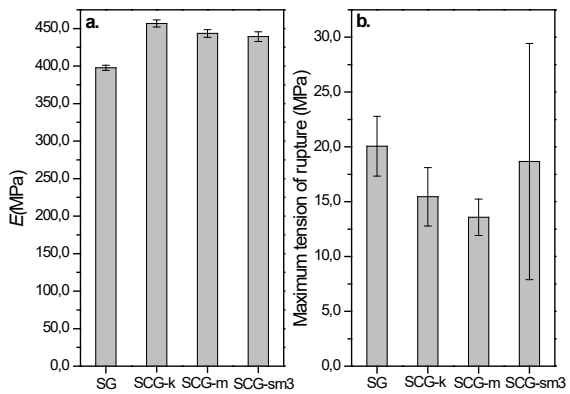

Figure 5. Mechanical strength test: a. Young's modulus (E) and b. ultimate tensile strength (σ_u) obtained from mechanical assays for the composites.

Studies, of similar systems to the evaluated in this article, have shown the most significant differences of the mechanical properties in relation to the films without addition of charge occur when adding 5-10% of kaolinite or montmorillonite [26-28], therefore, it is believed that higher load contents in the films evaluated would not present significant differences in relation to the values shown in Table 4.

The mechanical properties of cassava starch/glycerol films containing clay fillers were altered due to changes in crystallinity and changes in chain-chain interactions of the polymeric matrix [26]. The increase in the Young's modulus (E) observed in all films containing the different clay fillers (Table 4), indicates the interaction between the filler and the polymer matrix, providing greater rigidity to the material due to the increase in the number of hydrogen bonds [27].

The Young's modulus (E) and Ultimate Tensile Strength (σu) properties shown in Table 4 shown that the presence of montmorillonite and kaolinite clays increase the value of E and decrease the value σu, by comparation to the film without filler addition, therefore, the results obtained agree with the literature [26,27,29,30]. By the general comparation of the mechanical properties values previously discussed with those reported in the literature for similar systems, disregarding conditions of analysis such as conditioning and humidity of the samples, was observed that the obtained values shown in Table 4 are close to or higher than those reported, indicating the potential application of the films as food packaging [31-35]. More detailed studies on microbiological properties for such application of the evaluated materials have not been performed up to the moment.

In addition, the mean data shown in Table 4 were also submitted to statistical analysis of variance (ANOVA) and Tuckey Test, in order to establish if there was a statistically significant variation in the values presented between the analyzed materials.

Finally, the data obtained are not shown in the present work but, these have shown that the differences in Young's Modulus and Maximum Tensile Stress values are not statistically significant.

This suggest the hypothesis that the reinforcement levels incorporated into the films were not the more adequate, thus requiring the accomplishment of complementary studies seeking a greater variation of the load contents added to the films, in order to stipulate the optimal percentage of reinforcement for this system.

Figure 6 shows images of the synthesized films and their respective incorporated clay minerals.

Table 4. Thickness, Young's Modulus, Ultimate Tensile Strength and percentage change in relation to the SG film values.

Film	Thickness (mm)	Young's Modulus		Ultimate Tensile Strength	
		E **(MPa)**	**%*E***	**σ_u (MPa)**	**%σ_u**
SG	0.0801 ± 0.0074	397.64 ± 3.35	-	20.06 ± 2.72	-
SG-k	0.0809 ± 0.0069	456.66 ± 4.75	14.84	15.44 ± 2.65	-23.00
SG-m	0.0801 ± 0.0090	443.48 ± 5.17	11.53	13.58 ± 1.66	-32.28
SG-sm3	0.0824 ± 0.0185	439.26 ± 6.45	10.47	18.66 ± 10.77	-6.96

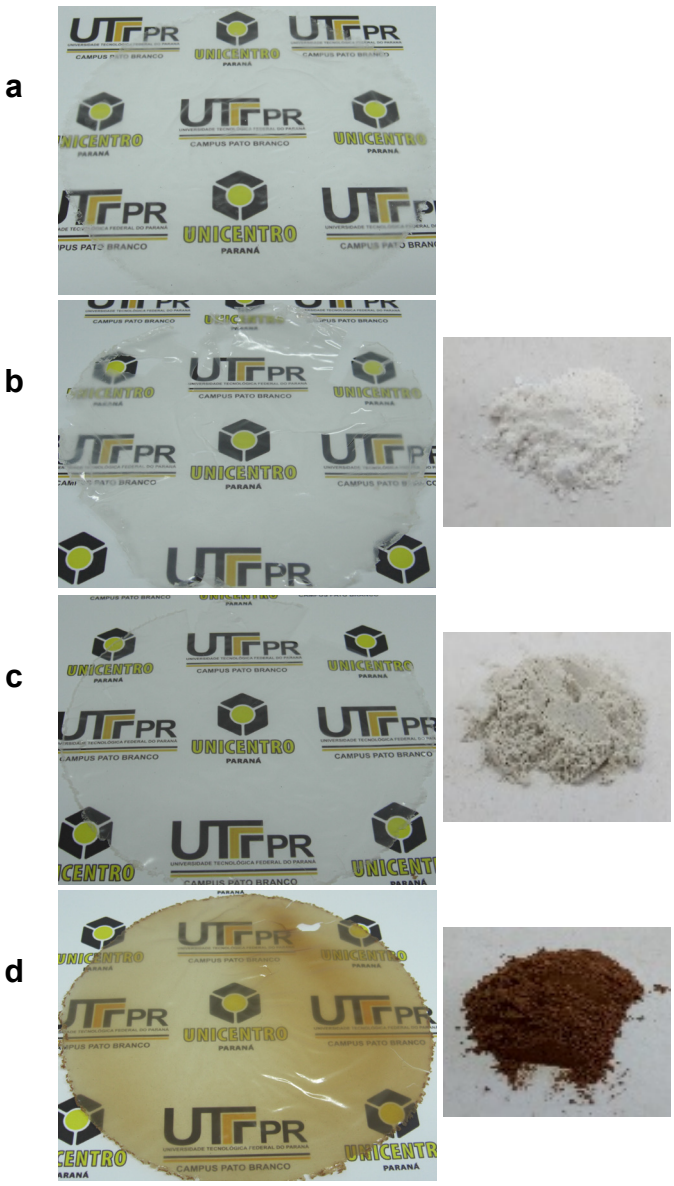

Figure 6. Images of the synthesized films and their respective clays added as fillers: a. SG; b. SG-k and (k); c. SG-m and (m); d. SG-sm3 and (sm3).

The images of Figure 6 shown that the only film that presented significant coloration difference due to the addition of clay as a filler was the SG-sm3 sample, Figure 6d, due to the reddish coloration of sm3 clay.

The optical properties of the films were evaluated by colorimetric analysis, the films were analyzed by the CIELAB system, where the parameters of brightness (L*), tendency for red or green (a*) and for yellow or blue (b*), hue angle (h) and chromaticity (C*) of the color were evaluated [36]. The effect of the presence of clay minerals were evaluated by the difference between the values measured in relation to the values obtained for the SG film, values of ΔL*, Δa*, Δb*, and these parameters were applied in determining the total color difference ΔE. The results are shown in Table 5.

Table 5. Colorimetric parameters of the films – values determined by the CIELAB system.

Parameter	SG	SG-k	SG-m	SG-sm3
L*	38.53	36.71	40.77	39.43
ΔL*	-	-1.82	2.24	0.90
a*	-1.32	-0.99	-0.90	-0.26
Δa*	-	0.33	0.42	1.06
b*	-0.15	-0.41	0.18	2.05
Δb*	-	-0.26	0.33	2.20
C*	1.35	1.07	0.92	2.06
h	185.99	202.44	168.93	97.67
ΔE	**-**	1.86	2.30	2.60

- data for the SG film.

In general, by the comparison to the SG film, the addition of the clays altered the colorimetric properties of the films. Due to the fact that the kaolinite and montmorillonite clays present themselves in white, they showed a low variation in the values of the color-related properties (a* and b*), but the SG-sm3 sample presented higher variations in these properties compared to the SG film, due to the red coloration of the clay, as shown in Figure 6. The red color acquired by the film is due to the presence of iron (Fe^{3+}) in the clay, which corroborates with what was observed in the FTIR and EDS analyses. This clay is also notable for the fact that it gives higher chromaticity (vivacity), while the other clays presented a lower result than the standard film in this parameter.

In relation to the total color difference (ΔE), the addition of kaolinite gave the lowest value, while the addition of montmorillonite led to a film with a clearer tendency, and the sm3 clay led to the greatest difference in total color, this film stands out for having been the only film that presented color differences, as observed in Figure 6.

The films were subjected to a water solubility test (%SM), and the results are shown in Table 6.

Table 6. Percentage of solubilized material (%SM) of films.

Film	%SM
SG	25.74 ± 2.10
SG-k	19.21 ± 4.07
SG-m	21.67 ± 5.30
SG-sm3	23.50 ± 4.97

The SG-k film presented the lowest solubility in water among all films evaluated. The addition of this clay increased the resistance of the film to degradations in the presence of water, this behavior is possibly due to the good interaction between the kaolinite and the polymer matrix by strong hydrogen bonds. For the solubility of the SG-m and SG-sm3 films, it is verified, considering the deviations of the measurements, that the obtained values are close to that of the SG film, indicating little effect of the addition of the montmorillonite and sm3 clays in this property.

3. Material and Methods

Precursors

The polymeric films were synthesized with the following precursors: cassava starch (Pinduca Indústria Alimentícia Ltda), glycerol (Alphatec - analytical grade) and the clay minerals, kaolinite (k) (extracted from the Rio Capim region, Pará State - Brazil), montmorillonite-SWy2 (m) (supplied by the American Clay Society) and the clay sample extracted in the city of São Miguel do Oeste – Santa Catarina State – Brazil (sm3), which is used by bricks industries. The sm3 filler was chosen because it had a red color and was composed of 44.51% montmorillonite, 26.18%

kaolinite, 5.03% hematite, among other polymorphous silica minerals (data obtained by analyses of X-ray diffraction, results not shown).

(Nano)composites Films Preparation

The (nano)composites films were prepared by the casting method and the methodology used for the synthesis of the films was adapted from the literature [37]. The films were obtained from the same concentration of cassava starch (9.0 g - 3 wt/vol % in relation to the initial solution volume - 300 mL of deionized water) and of clay minerals (0.09 g - 5 wt/wt % in relation to starch mass). The glycerol was added as a plasticizer agent (2.7 g - 30 wt/wt % relative to starch mass).

Initially, the amounts of glycerol and clay minerals were added to 300 mL of distilled water, next, the mixture was placed in an ultrasonic bath for 60 min, after this time, the starch was added to the mixture and the total volume of the solution was adjusted to 400 mL by the addition of distilled water. The solution was submitted magnetic agitation for homogenization. After the homogenization of the components, the solution was subjected to the gelatinization process under heating at 70 °C and constant mechanical stirring for 20 minutes, after, the mixture remained under stirring until cooled to room temperature. The filmogenic solution was placed in the ultrasonic bath for 60 min for the removal of gas bubbles.

With the aid of a semi-analytical balance, portions of 65 g of the filmogenic solution were transferred to glass Petri dishes with a diameter of 15 cm, which were subjected to heating at 45 °C in a forced air oven, for 36 h. After evaporation of the water, the dishes containing the films were placed in a desiccator containing 1 L of distilled water (at room temperature), where the samples remained for 5 days. This step had the purpose of promoting the detachment of the films from the glass dishes.

Thickness

The thickness of the films was determined with an Insize digital micrometer (1-25 mm) with an accuracy of 0.001 mm. Six measurements were performed on each sample, discarding the outlier value. The remaining values were treated statistically by calculating the mean and standard deviation.

Fourier Transform Infrared Spectroscopy - FTIR

FTIR analyses were performed on a Frontier Perkim-Elmer spectrometer, through the attenuated total reflectance (ATR) and diamond crystal method. The FTIR spectra were obtained in the range of 4000-400 cm^{-1}, with a resolution of 4 cm^{-1} and accumulation of 32 scans.

X-Ray Diffractometry - XRD

Measurements of X-ray diffraction were obtained in a Rigaku diffractometer model MiniFlex 600, with CuKα (λ = 1.5418 Å) operating at 40 kV voltage and 15 mA current, at a speed of 4° min^{-1} and step of 0.02°. The clays and the polymeric films was deposited in the glass sample holder.

Scanning Electron Microscopy - SEM

Scanning electron microscopy analyses was carried out at 15 kV using a Hitachi scanning electron microscope, model TM3000, with a tungsten filament source. Each sample was deposited on carbon tape on an aluminum stub.

Chemical Analysis by Energy-Dispersive Spectroscopy - EDS

Quantitative chemical analyses by energy-dispersive spectroscopy (EDS) were performed using a Hitachi TM3000 scanning electron microscope coupled with a SwiftED3000 (EDS) detector, operating at 15 kV, and a tungsten filament source with 1000x magnification. The results are expressed as the atomic percentage of the elements present in the samples.

Thermogravimetric Analysis

The thermal analyses were performed on TA Instruments thermal analyzer model SDT Q-600, with the samples placed in alumina crucibles. The analyses were performed in the temperature range of 30 to 800 °C, with a heating ramp of 10

°C min^{-1}, under nitrogen atmosphere with a flow of 30 mL min^{-1}.

Mechanical Resistance Analysis

The mechanical properties were obtained in tensile mode by the use of an EMIC DL-3000 universal assay apparatus, equipped with a load cell of 5 kN. Five samples were tested for each composition. The samples were kept under controlled humidity conditions (43% relative air humidity) for 1 week, using a saturated solution of K_2CO_3 and average values were considered. The testing room was kept at 43±1% relative humidity and 25±1 °C. The samples were cut into 1 cm x 8 cm ribbons with average thickness of 0.08 mm. The initial distance (gauge length) between the instrument grips was kept at 30 mm, and the samples were tested at a cross-head speed of 30 mm min^{-1}. Using the obtained stress versus strain curves, Young's modulus (E) (from curve fitting in the initial linear section until 1% deformation by the least-squares method) and ultimate tensile strength (σu) were calculated. The methodology was adapted from ASTM D882-02.

Colorimetric Analysis

The colorimetric analyses of the films samples were performed in a Konica Minolta CR-400 portable colorimeter, equipped with a dark chamber to avoid possible interferences in the readings. The CIELAB System was adopted for interpretations of the measures.

The effect of the presence of the clay minerals on the color of the films compared to the pure film (SG) was performed by the total color difference ΔEab, determined by Equation 1:

$$\Delta Eab = [(\Delta L)^2+(\Delta a)^2+(\Delta b)^2]^{1/2} \quad (1)$$

Where ΔEab is the total color difference, ΔL the difference between light and dark, Δa the difference between red and green and Δb the difference between yellow and blue [36].

Water solubility

The water solubility of the films was determined by methodologies adapted from the literature [38, 39]. The procedure was performed in triplicate. Strips of 4 cm^2 of the films were cut and dried in an oven at 45 °C for 30 minutes, then the mass of the films was measured on an analytical balance and they were deposited in properly tared Petri dishes. The system was allowed to stand out for 24 hours after adding 30 mL of water to the dishes, then the water was removed with a micropipette and the films were dried in a forced air oven (105 °C - 24 hours). After drying, the dried films were again weighed and the content of solubilized material was obtained by Equation 2.

$$\%SM = (mf-mi)/mi \times 100 \quad (2)$$

Where, %SM is the percentage of solubilized material, mf is the final mass and mi is the initial mass of the sample.

4. Conclusions

The presence of the clay minerals in the polymer matrix was verified by the FTIR, SEM and EDS analyses. No formation of new phases between a polymer matrix and clays was identified by the XRD technique. The SG-k sample stands out in this analysis, since basal reflections, characteristic of kaolinite, were identified, they are displaced at the lowest angles of diffraction due, possibly, to the interactions of the clay with the polymer matrix.

In relation to the characterizations that reflect in the application of the films, the addition of the clay minerals, in general, led to lower temperatures of thermal degradation, different optical properties and improvements in the mechanical properties, showing greater capacity of elongation and lower rupture tensions.

The addition of kaolinite as a filler stood out among the evaluated clay minerals, as it led to greater differences in relation to the SG film for the thermal and mechanical properties and showed higher resistance to water solubility compared to other clay minerals.

The obtained results shown that the obtained films present changes in the properties, are possible to apply, present low cost, and are obtained only with precursors of natural origin, impacting in the reduction of environmental problems in disposal.

Acknowledgments

The authors are grateful to the following brazilian funding agencies for financial support: CNPQ (grant 404392/2016-4) and CAPES, for providing scholarship to our graduate student. The authors wish to thank the UTFPR/Guarapuava for the mechanical traction essays.

References and Notes

[1] Anadão, P.; Wiebeck, H.; Valenzuela-Díaz, F. R. *Polímeros* **2011**, *21*, 443.

[2] Fiori, A. P. S. M.; Gabiraba, V. P.; Praxedes, A. P. P.; Nunes, M. R. S.; Balliano, T. L.; Silva, R. C.; Tonholo, J.; Ribeiro, A. S. *Polímeros* **2014**, *24*, 628.

[3] Schlemmer, D. A.; Carvalho, L. A.; Valadares, L. F. In Embrapa Agroenergia - *Comunicado Técnico Embrapa*, Brasília **2014**.

[4] Arjmandi, R.; Hassan, A.; Haafiz, M. K. M.; Zakaria, Z. *Fibers Polym.* **2015**, *16*, 2284.

[5] Tripathi, N.; Katiyar, V. J. *J. Appl. Polym. Sci.* **2016**, [Crossref]

[6] Lu, D. R.; Xiao, C. M.; Xu, S. J. *Express Polym. Lett.* **2009**, *3*, 366.

[7] Shimazu, A. A.; Mali, S.; Victória, M. V. E. *Semin. Ciências Agrárias* **2007**, *28*, 79.

[8] Ortiz, J. A. R.; Moro, T. A., Maria, E.; Lima, B.; Carvalho, W. P. Análise do perfil de cristalinidade e microestrutura de bioplásticos de amidos adicionados de vermiculita. VII Workshop de Nanotecnologia Aplicada ao Agronegócio. *Embrapa Instrumentação*, **2013**, 103.

[9] Botan, R.; Gonçalves, N. A.; Moraes, S. B.; Lona, L. M. F. *Polímeros* **2015**, *25*, 117.

[10] Mali, S.; Grossmann, M. V. E.; Yamashita, F. *Semin. Ciências Agrárias* **2010**, *31*, 137.

[11] Callister Jr., W. D.; Rethwisch, D. G. Fundamentals os Materials Science and Engineering: Na Integrated Approach, Fourth Edition, John Wiley and Sons, New York, USA, 2012, 566.

[12] Coelho, A. C. V.; Santos, P. S.; Santos, H. S. *Quim. Nova* **2007**, *30*, 146.

[13] Teixeira-Neto, É.; Teixeira-Neto, Â. A. *Quim. Nova* **2009**, *32*, 809.

[14] Balau, L.; Lisa, G.; Popa, M. I.; Tura, V.; Melnig, V. *Cent. Eur. J. Chem.* **2004**, *2*, 638.

[15] Yu, J.; Yang, J.; Liu, B.; Ma, X. *Bioresour. Technol.* **2009**, *100*, 2832.

[16] Râpă, M.; Grosu, E.; Stoica, P.; Andreica, M.; Hetvary, M. J. *Environ. Res. Prot.* **2014**, *11*, 34.

[17] Wijesinghe, J. A. A. C.; Wicramasinghe, I.; Saranandha, K. H. *Am. J. Food Sci. Technol.* **2015**, *3*, 10.

[18] Gardolinski, J. E.; Martins Filho, H. P.; Wypych, F. *Quim. Nova* **2003**, *26*, 30.

[19] Temuujin, J.; Jadambaa, T.; Burmaa, G., Erdenechimeg, S.; Amarsanaa, J.; MacKenzie, K. J. D. *Ceram. Int.* **2004**, *30*, 251.

[20] Madejová, J.; Pentrák, M.; Pálková, H.; Komadel, P. *Vib. Spectrosc.* **2009**, *49*, 211.

[21] Perotti, G. F.; Tronto, J.; Bizeto, M. A.; Izumi, C. M. S.; Temperini, M. L. A.; Lugão, A. B.; Parra, D. F.; Constantino, V. R. L. *J. Braz. Chem. Soc.* **2014**, *25*, 320.

[22] Biscaye, P. E. *Am. Mineral.* **1964**, *49*,1282.

[23] Tsunematsu, K.; Tateyama, H. *J. Am. Ceram. Soc.* **1999**, *82*, 1589.

[24] Machado, B. A. S.; Reis, J. H. O.; Da Silva, J. B.; Cruz, L. S.; Nunes, I. L.; Pereira, F. V.; Druzian, J. I. *Quim. Nova* **2014**, *37*, 1275.

[25] Wilhelm, H. M.; Sierakowski, M. R.; Souza, G. P.; Wypych, F. *Polymer International* **2003**, *52*,1035.

[26] Mbey, J. A.; Hoppe, S.; Thomas, F. *Polymer Composites* **2015**, 186.

[27] Carvalho, A. J. F.; Curvelo, A. A. S.; Agnelli, J. A. M. *Carbohydr. Polym.* **2001**, *45*, 189.

[28] Mbey, J. A.; Hoppe, S.; Thomas, F. *Carbohydr. Polym.* **2012**, *88*, 213.

[29] Monteiro, M. K. S.; Oliveira, V. R. L.; Santos, F. K. G.; Leite, R. H. L.; Aroucha, E. M. M.; Silva, R. R., Silva, K. N. O. *Mater. Res. (Sao Carlos, Braz.)* **2017**, *20*, 69.

[30] Meite, N.; Konan, L. K.; Bamba, D.; Goure-Doubi, B. I. H.; Oyetola, S. *Mater. Sci. Appl.* **2018**, *9*, 41.

[31] Costa, S. S.; Druzian, J. I.; Machado, B. A. S.; Souza, C. O.; Guimarães, A. G. *Plos One* **2014**, 9.

[32] Souza, A. C.; Benze, R.; Ferrão, E. S.; Ditchfield, C.; Coelho, A. C. V.; Tadini, C. C. *Food Sci. Technol.* **2012**, *46*, 110.

;[33] Borges, J. A.; Romani, V. P.; Cortez-Vega, W. R.; Martins, V. *Int. Food Res. J.* **2015**, *22*, 2346.

[34] Iamareerat, B.; Singh, M.; Sadiq, M. B.; Anal, A. K. *J. Food Sci. Technol.* **2018**.

[35] Shah, U.; Gani, A.; Ashwar, B. A.; Shah, A.; Ahmad, M.; Gani, A.; Wani, I. A.; Masoodi, F. A. *Cogent Food Agric.* **2015**, *1*, 1115614.

[36] Konica Minolta Sensing Americas, Entendendo o Espaço de Cor L*a*b* <http://sensing.konicaminolta.com.br/2013/11/entendendo-o-espaco-de-cor-lab/>, access:09/15/2017.

[37] Silva, M. L. N.; Marangoni, R.; Silva, A. H.; Wypych, F.; Schreiner, W. H. *Polímeros* **2013**, *23*, 248.

[38] Gontard, N.; Duchez, C.; Cuq, J.-L.; Guilbert, S. *Int. J. Food Sci. Technol.* **1994**, *29*, 39.

[39] Nazan, K. T.; Şahbaz, F. *J. Food Eng.* **2004**, 61, 459.